

# High-resolution solid-state $^{13}\text{C}$ n.m.r. study of isotactic polypropylene gel

Takahiko Nakaoki\*, Hironori Shuto, Hisao Hayashi and Ryoza Kitamaru  
 Faculty of Science and Technology, Ryukoku University, Seta Otsu 520-21, Japan  
 (Received 26 September 1997; revised 4 November 1997; accepted 3 December 1997)

The molecular conformational structure of isotactic polypropylene (iPP)/*o*-dichlorobenzene gel is investigated by means of solid-state high-resolution  $^{13}\text{C}$  n.m.r. spectroscopy. It was revealed from the resonance line of methylene carbon at the position generating one  $\gamma$ -*gauche* effect that the gel-forming crystal takes a 3/1 helical molecular conformation. However, the resonance lines observed for the gel were very broad. In order to deconvolute overlapping peaks, the Lorentzian type peak was converted to Gaussian one by computational analysis. The crystalline component of the resonance line consists of two peaks, of which the chemical shifts were identified with those for the  $\alpha$ -iPP crystal. However, the peak intensity ratio of the downfield line to the upfield one in the gel, 1:2, was opposite to the 2:1 ratio in the  $\alpha$ -iPP crystal usually reported for melt crystallised films. This is thought to be due to the difference of interchain interaction within the crystal cell. The crystal structure and the crystallinity of the gel were independent of the polymer concentration. The gel-forming crystal did not take a polymer–solvent complex as in the case of polystyrene gel. © 1998 Published by Elsevier Science Ltd. All rights reserved.

(Keywords: isotactic polypropylene; solid state  $^{13}\text{C}$  n.m.r.; gel)

## INTRODUCTION

The gelation for crystalline polymer generally accompanies the formation of crystalline entity as a cross-linking point. Therefore the gelation process is regarded as a kind of crystallisation from polymer solutions. Solid-state high-resolution  $^{13}\text{C}$  n.m.r. spectroscopy is well known to be a powerful technique for investigating the molecular structure of crystalline polymers. The chemical shift of methylene carbon provides good information on the molecular structure of vinyl polymer. That is, the upfield shift of *ca.* 5 ppm due to  $\gamma$ -*gauche* effect<sup>1</sup> and the split due to interchain interaction<sup>2</sup> are expected to characterise the crystal modification. Based on the above concept, we have investigated the molecular structure and phase structure of syndiotactic polypropylene (sPP)/*o*-dichlorobenzene gel by means of solid-state high-resolution  $^{13}\text{C}$  n.m.r. spectroscopy<sup>3,4</sup>. It was found that the methylene resonance in the sPP gel splits into three components which are completely different from the peak profile of bulk crystals reported before<sup>5–8</sup>. This was explained by the split due to both of the  $\gamma$ -*gauche* effect induced by taking *trans*–*trans*–*gauche*–*gauche* sequence and the interchain packing effect. The phase structure was also investigated by curve-fitting analysis and spin-lattice relaxation behaviour. Semicrystalline polymers are generally composed of domains with different chain mobility; crystalline, noncrystalline and interphase between crystalline and noncrystalline. The molecular chains close to the crystalline surface are somewhat ordered but considerably mobile. Some solvent molecules were strongly bound in the interphase domain so that the molecular mobility is restricted.

Isotactic polypropylene (iPP) is another stereoregular counterpart of sPP. This polymer is known to take three kinds of crystalline forms in a bulk crystallised state; monoclinic ( $\alpha$ -form)<sup>9</sup>, trigonal ( $\beta$ -form)<sup>10–16</sup> and

orthorhombic ( $\gamma$ -form)<sup>17–20</sup> cells. In regard to the molecular conformation of iPP, all crystal modifications adopt a *trans*–*gauche* sequence (3/1 helix). A detailed n.m.r. investigation of the  $\alpha$ -iPP crystal was carried out by Bunn *et al.*<sup>2</sup>. They pointed out that the splitting in the methyl and methylene resonances interpreted in terms of the two inequivalent environments was identified for the monomeric unit. However, as for the gel, there has been no investigation on molecular structure. This paper deals with the computational analysis of the spectral feature of iPP observed for the gel prepared by solutions with various concentration by converting from Lorentzian to Gaussian function. In addition, the feature of the gels structure is discussed in comparison with that of melt-crystallised films.

## EXPERIMENTAL

The iPP samples were provided by Showa Denko Co. Ltd. They were purified by soxlet extraction with *n*-heptane. The meso triad was estimated to be 98.5% by  $^{13}\text{C}$  n.m.r. The solvent used for gelation was *o*-dichlorobenzene. Both polymer and solvent were placed in an ampoule and degassed in vacuo. The homogenised solutions were prepared by heating the well-blended polymer/solvent mixture at 150°C for 30 min, and quenched into iced water to obtain the gel. The resultant gels were maintained in iced water for 30 min. The  $\alpha$ -iPP crystal was obtained by the isothermal crystallisation at 130°C for 24 h after melting at 230°C.

Solid-state high-resolution  $^{13}\text{C}$  n.m.r. spectra were taken with a Bruker MSL 200 spectrometer at a field strength of 4.7 T. The  $^{13}\text{C}$  chemical shifts were obtained with respect to the signal of tetramethylsilane (TMS). The magic angle spinning (MAS) of 3 kHz was achieved by the double bearing system. The desired accumulation time was varied by gel concentration. To avoid the broadening of signals, we did not use any window functions except the Lorentzian–Gaussian conversion analysis. Spin-lattice relaxation time ( $T_{1c}$ ) was measured by saturation recovery method. The

\* To whom correspondence should be addressed

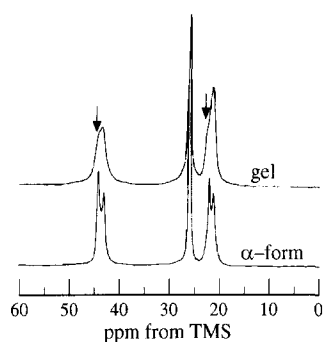


**Figure 1** CP/MAS  $^{13}\text{C}$  n.m.r. spectra of iPP/o-dichlorobenzene gel (14 wt%) and  $\alpha$ -iPP crystal

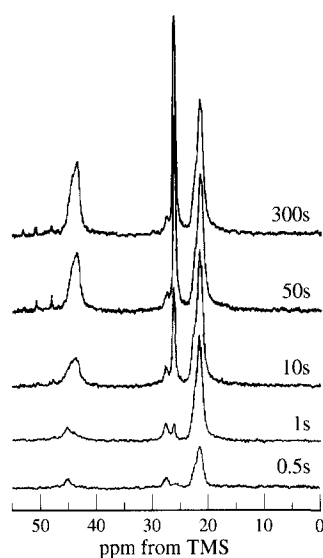


**Figure 2** Actual spectra in the time progression of the saturation recovery ( $T_{1C}$  relaxation) of iPP/o-dichlorobenzene gel (14 wt%). The recycle delays are drawn in the spectra

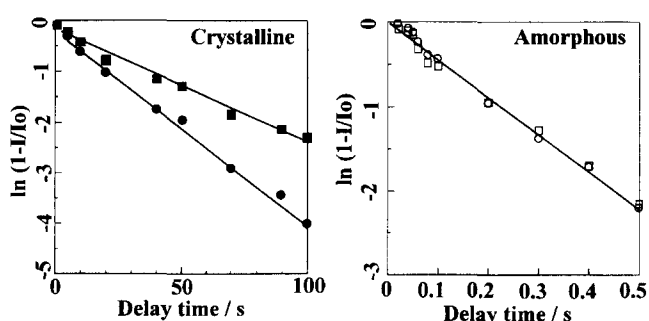


**Figure 3**  $^{13}\text{C}$  spin-lattice relaxation process for methylene (■) 43.3 ppm; (□) 45.1 ppm and methine (●) 26.0 ppm; (○) 27.4 ppm carbons

**Table 1**  $T_{1C}$  values for methylene and methine carbons in the iPP/o-dichlorobenzene gel (14 wt%)

	Chemical shift (ppm)	$T_{1C}$ (s)	Assignment
CH <sub>2</sub>	45.1	0.2	Amorphous
	43.3	48	Crystalline
CH	27.4	0.2	Amorphous
	26.0	24	Crystalline

computational analysis was achieved by 1D-WINNMR software from Bruker.

Thermal analysis was performed by a Rigaku TAS 200 differential scanning calorimeter (d.s.c.). The samples were scanned at heating and cooling rates of 1, 3, and 5°C/min.

The transition enthalpy was estimated by extrapolation to the rate of 0°C/min in order to eliminate the influence of heating and cooling rate.

## RESULTS AND DISCUSSION

### $^{13}\text{C}$ n.m.r. spectral shape of the iPP gel

Figure 1 shows the cross polarisation (CP)/MAS  $^{13}\text{C}$  n.m.r. spectra of the iPP/o-dichlorobenzene gel (14 wt%) and the  $\alpha$ -iPP crystal. The spectra consist of three regions of signals due to methylene, methine and methyl carbon groups from downfield. The spectra is not similar to the profile of the  $\alpha$ -form rather than that of the  $\beta$ -form<sup>2</sup>. Namely, a clear doublet in the methylene and methyl resonances characteristic to the  $\alpha$ -iPP crystal was not observed in the gel. Detailed observation, however, reveals that the line shape of the gel is a little different from the  $\beta$ -form, i.e. as shown by arrows in Figure 1, it is featured by methylene and methyl resonances with a downfield shoulder. As described in Section 1, the  $\gamma$ -gauche effect for methylene resonance gives important information on conformational structure. Since the chemical shift of methylene resonance in Figure 1(a) is around 44 ppm, which is common to all the crystal modifications of iPP, the *trans*-gauche sequence generating one  $\gamma$ -gauche effect is formed in the gel. The spectral change observed by the saturation recovery pulse sequence is shown in Figure 2. For the methylene and methine peaks, the noncrystalline component having good mobility at 45.1 and 27.4 ppm was measured in shorter delay time. The relaxation behaviours for methylene and methine carbons are shown in Figure 3, and the estimated  $T_{1C}$  values are listed in Table 1. The  $T_{1C}$  values for the amorphous component were around 0.2 s, but those for the crystalline component were in the order of some tens of seconds. The longer relaxation time in the gel is compatible with that of the  $\alpha$ -iPP crystal. This result suggests that the rigid domain of crystal is constructed in the gel.

Although a peak broadening induced by dipole-dipole interaction and chemical shift anisotropy is eliminated in the solid-state high-resolution  $^{13}\text{C}$  n.m.r. spectrum by combination of dipolar decoupling and MAS technique, the resolution is not good enough compared with the liquid  $^{13}\text{C}$  n.m.r. spectrum. In some cases, the overlapping peaks, which are often represented by Lorentzian function are difficult to distinguish. In order to get higher resolution, narrower signals can be better obtained by converting from Lorentzian to Gaussian function. The observed intensity  $E(\nu)$  at  $\nu$ , is described by the following Lorentzian function

$$E(\nu) = \frac{\sigma/\pi}{\sigma^2 + \nu^2} * \delta(\nu - \nu_0) \quad (1)$$

where  $\sigma$  and  $\nu_0$  are the half width and the peak positions, respectively. The notation \* represents the convolution between Lorentzian and  $\delta$  functions. Fourier transformation of  $E(\nu)$  leads to the free induction decay (FID) shown as

$$\int_{-\infty}^{\infty} E(\nu) \exp(2\pi i \nu t) d\nu = \exp(2\pi \sigma |t|) \cos(2\pi \nu_0 t). \quad (2)$$

This relation can be rearranged to

$$\int_{-\infty}^{\infty} E(\nu) \exp(2\pi i \nu t) d\nu \exp(-2\pi \sigma |t|) = \cos(2\pi \nu_0 t). \quad (3)$$

For the actual n.m.r. measurement, the time to get the data point is restricted to a few milliseconds. Therefore, by using the window function  $A(t)$ , Fourier transformation of FID can

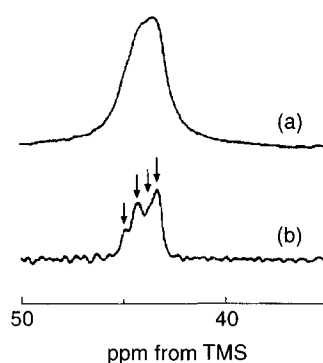


**Figure 4** CP/MAS  $^{13}\text{C}$  n.m.r. spectrum of iPP/o-dichlorobenzene gel (14 wt%) (a) and the result converted from Lorentzian to Gaussian functions (b)

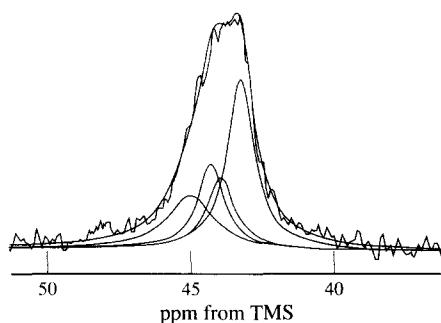


**Figure 5** Curve-fitting analysis of methylene carbon in the fully relaxed  $^{13}\text{C}$  n.m.r. spectrum of iPP/o-dichlorobenzene gel (14 wt%). The assignments are shown in Table 2

**Table 2** The result of curve-fitting analysis for methylene carbon in the gel

Chemical shift (ppm)	Fraction	Assignment
45.1	0.21	Amorphous
44.3	0.20	Crystalline
44.0	0.19	Interphase
43.3	0.40	Crystalline

be rewritten as

$$\begin{aligned}
 & \int_{-\infty}^{\infty} \int_{-\infty}^{\infty} A(t) E(\nu) \exp(2\pi i \nu t) \exp(-2\pi \sigma |t|) \\
 & \quad \exp(2\pi i \nu t) dt d\nu \quad (4) \\
 & = \int_{-\infty}^{\infty} A(t) \cos(2\pi \nu_0 t) \exp(2\pi i \nu t) dt \\
 & = \int_{-\infty}^{\infty} A(t) \exp(2\pi i \nu t) dt * \delta(\nu - \nu_0)
 \end{aligned}$$

This equation indicates that the line shape is characterised by the Fourier transformation of the window function  $A(t)$ . In this analysis, we used the Gaussian function as  $A(t)$ . In order to carry out this procedure, the actual spectrum requires a good signal to noise ratio. So we applied this analysis to the FID accumulated over 40 000 times by CP/MAS method. Figure 4 shows the observed CP/MAS  $^{13}\text{C}$  n.m.r. spectrum and the result of conversion to Gaussian function for the methylene carbon. As shown in this chart, the resonance line is decomposed to three peaks and a

shoulder. Two peaks at 43.3 and 44.3 ppm provide the same chemical shift to those of the  $\alpha$ -iPP crystal. The most downfield peak at 45.1 ppm is the contribution from the amorphous as described in  $T_{1\rho}$  analysis. According to Kitamaru and co-workers, the shoulder at 44.0 ppm is attributed to the contribution from the interphase component<sup>21</sup>. By using these four resonance lines, we attempted the curve-fitting analysis in order to evaluate the phase fraction. However, the CP/MAS  $^{13}\text{C}$  n.m.r. spectrum was not suitable for quantifying the phase fraction because of different CP efficiencies among different phases depending on molecular mobility. The pulse program with long enough waiting time (over 5 times longer than the longest  $T_{1\rho}$ ) after the  $90^\circ$  single pulse allows us to evaluate the relative fraction. Figure 5 shows the single-pulse  $^{13}\text{C}$  n.m.r. spectra without CP of the iPP/o-dichlorobenzene gel. Since the waiting time is 300 s, which is enough to recover all the magnetisation used, these spectra reflect both the crystal and the amorphous components. The result of curve-fitting analysis of methylene resonance in the gel is also shown in Figure 5. The integral intensity ratio of the peak at 43.3 ppm to that at 44.3 ppm was 2:1. However, this ratio is opposite to the ratio of 2:1 reported for the  $\alpha$ -iPP crystal<sup>2</sup>. The splitting in the methylene resonance of the  $\alpha$ -iPP crystal reflects the inequivalent environment that exists in the monoclinic unit cell. Therefore, it is concluded that the chain arrangement within the crystal unit cell for the present gels is different from the  $\alpha$ -iPP crystal. Determination of the chain arrangement within the crystal unit cell must be done by X-ray diffraction analysis in further structural investigation. The deconvolution procedure allows us to estimate the phase fraction. Each fraction evaluated by integral intensity is summarised in Table 2. The crystallinity in the gel is ca. 0.6, which is almost the same as that of the bulk-crystallised  $\alpha$ -iPP<sup>21</sup>. Although the gel includes a considerable amount of crystalline component, we must emphasise that this value is too high to justify as the fraction required for the initial stage of gelation, but is acceptable as the fraction for the later state after holding for a long time.

#### Molecular structure and crystallinity in various concentration

To study the gelation mechanism in relation to the concentration, single-pulse  $^{13}\text{C}$  n.m.r. spectra of iPP/o-dichlorobenzene gel were observed for the specimens prepared from three kinds of concentrations which is shown in Figure 6. These spectra reflect both crystalline and noncrystalline components. Interestingly, there is no difference in spectral shape among them, indicating that the same molecular structure is constructed in the gel. The relative intensity for the amorphous phase at 27.4 ppm against the crystalline phase at 26.0 ppm is the same, independent of the concentration. This confirms that the fraction of crystal phase within the gel remains unchanged. To check this, d.s.c. measurements were carried out to get further information on the crystallinity. Figure 7 shows the d.s.c. curve for the iPP/o-dichlorobenzene gel (14 wt%), which displays a broad endothermic peak at  $117^\circ\text{C}$  corresponding to the gel melting. In Figure 8, the gel-melting enthalpy is plotted against concentration. The values estimated increase linearly as the polymer concentration increases. This linear relationship suggests that the crystallinity of the gels is constant. In the case of isotactic polystyrene gel, Guenet and co-workers showed that the gel-melting enthalpy increases with increasing polymer concentration at first, but decreases gradually with further

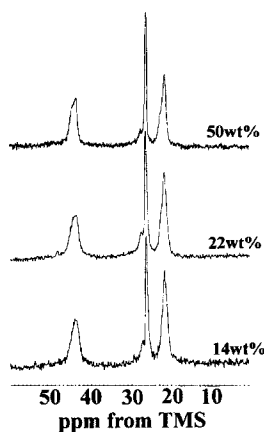


**Figure 6** Single pulse  $^{13}\text{C}$  NMR spectra of iPP/o-dichlorobenzene gel with polymer concentration of 50, 22, and 14 wt%. The waiting time of 300 s is enough time to provide the thermoequilibrium state

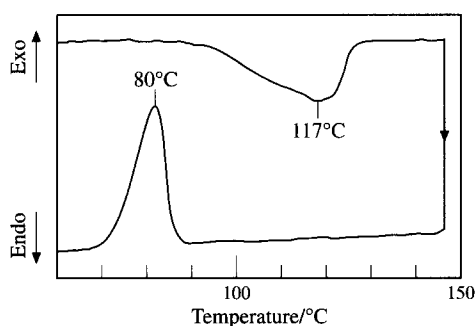


**Figure 7** D.s.c. thermogram of iPP/o-dichlorobenzene gel (14 wt%). Heating and cooling rate was  $5^\circ\text{C}/\text{min}$

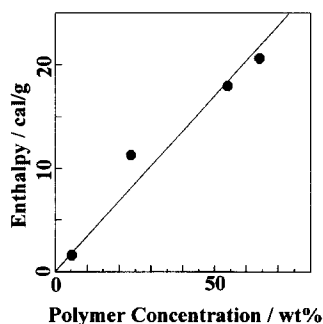


**Figure 8** Gel-melting enthalpy depending on polymer concentration

increasing of the concentration<sup>22–24</sup>. They concluded that the formation of a polymer–solvent complex or a stoichiometric compound gives the maximum enthalpy. The iPP gel showed the different behaviour from the iPS gel. That is, during the crystallisation process to form gel, the solvent molecules were excluded from the crystalline domain. The difference of gelation mechanism between iPP and iPS will be understood by the bulkiness of side group. The phenyl group will have enough space for the solvent molecule to enter into the crystal cell.

#### Conclusions

The iPP makes a thermoreversible physical gel by forming the crystalline as a network structure. Although

the broad peaks of iPP/o-dichlorobenzene gel observed in solid-state high-resolution  $^{13}\text{C}$  n.m.r. spectrum made difficult to interpret the molecular structure, the analysis of Lorentzian–Gaussian conversion provided important information. The existence of four peaks for methylene carbon was clear. Among the four peaks, the two peaks at 43.3 and 44.3 ppm were contributed by the crystalline phase, and the other two peaks appearing at 45.1 and 44.0 ppm were from amorphous and interphase components. The peak positions of crystalline component were the same as those observed in the  $\alpha$ -iPP crystal. However it should be noted that the integral intensity ratio of 1:2 observed for the peaks at 43.3 and 44.3 ppm is opposite to the bulk-crystallised  $\alpha$ -iPP. Calculations of crystalline content using the single-pulse  $^{13}\text{C}$  n.m.r. spectra and d.s.c. showed that the crystallinity was almost constant in the concentration range from 14 to 64 wt%.

#### ACKNOWLEDGEMENTS

This work was supported in part by the Science Research Promotion Fund of Japan Private School Promotion Foundation.

#### REFERENCES

1. Tonelli, A. E. and Schilling, F. C., *Acc. Chem. Res.*, 1981, **14**, 233.
2. Bunn, A., Cudby, M. E. A., Harris, R. K., Packer, K. J. and Say, B. J., *Polymer*, 1982, **23**, 694.
3. Nakaoki, T., Hayashi, H. and Kitamaru, R., *Polymer*, 1996, **37**, 4833.
4. Nakaoki, T. and Kitamaru, R., *Rep. Prog. Polym. Phys. Jpn.*, 1994, **37**, 537.
5. Bunn, A., Cudby, M. E. A., Harris, R. K. and Say, B. J., *Chem. Soc., Chem. Commun.*, **1981**, 15.
6. Sozzani, P., Galimberti, M. and Balbontin, G., *Makromol. Chem., Rapid Commun.*, 1992, **13**, 305.
7. Sozzani, P., Simonutti, R. and Galimberti, M., *Macromolecules*, 1993, **26**, 5782.
8. Asakura, T., Aoki, A., Date, T., Demura, M. and Asanuma, T., *Polymer J.*, 1996, **28**, 24.
9. Natta, G. and Corradini, P., *Nuovo Cimento Suppl.*, 1960, **15**, 40.
10. Hsu, C. C. and Geil, P. H. J., *Polym. Sci., Polym. Phys. Ed.*, 1986, **24**, 2379.
11. Grubb, D. T. and Yoon, D. Y., *Polym. Commun.*, 1986, **27**, 84.
12. Corradini, P., Petraccone, V., De Rosa, C. and Guerra, G., *Macromolecules*, 1986, **19**, 2699.
13. Corradini, P., De, R., Guerra, G. and Petraccone, V., *Polym. Commun.*, 1989, **30**, 281.
14. Yan, R. J., Li, W., Li, G. and Jiang, B., *Macromolecular Sci. Phys.*, 1993, **B32**, 15.
15. Gomez, M. A., Tanaka, H. and Tonelli, A. E., *Polymer*, 1987, **28**, 2227.
16. Meille, S. V., Ferro, D. R., Brukner, S., Lovinger, A. L. and Padden, F. J., *Macromolecules*, 1994, **27**, 2615.
17. Meille, S. V., Brukner, S. and Porzio, W., *Macromolecules*, 1990, **23**, 4114.
18. Brukner, S., Meille, S. V., Sozzani, P. and Torri, G., *Makromol. Chem., Rapid Commun.*, 1990, **11**, 55.
19. Campbell, R. A., Phillips, P. J. and Lin, J. S., *Polymer*, 1993, **34**, 4809.
20. Brukner, S. and Meille, S. V., *Nature*, 1989, **340**, 455.
21. Saito, S., Moteki, Y., Nakagawa, M., Horii, F. and Kitamaru, R., *Macromolecules*, 1990, **23**, 3256.
22. Guenet, J. M., *Macromolecules*, 1986, **19**, 1961.
23. Guenet, J. M. and McKenna, G. B., *Macromolecules*, 1988, **21**, 1752.
24. Guenet, J. M. and Klein, M., *Makromol. Chem., Macromol. Symp.*, 1990, **39**, 85.